Resonant-Coherent Excitation of Channeled Ions

F. J. García de Abajo
Departamento de CCIA, Facultad de Informática,
Universidad das País Vasco/Euskal Herriko Unibersitatea,
Aptdo. 649, 20080 San Sebastián, Spain

P. M. Echenique
Departamento de Física de Materiales, Facultad de Química,
Universidad das País Vasco/Euskal Herriko Unibersitatea,
Aptdo. 1072, 20080 San Sebastián, Spain
(Received 25 October 1995)

A first-principles calculation of the resonant-coherent excitation of planar-channeled hydrogenic ions is presented. The interplay between coherent interaction with the periodic crystal lattice potential and inelastic electron-electron collisions is shown to be crucial in both intraionic transitions and electron loss from the ion. The magnitude of resonant-coherent excitation is predicted to oscillate with the amplitude of the oscillations of the ion trajectory. Good agreement is found with experiments.

PACS numbers: 61.85.+p, 34.50.Fa, 34.80.Dp, 79.20.–m

A channeled ion moving inside a crystal is exposed to the periodic perturbation of the ordered rows and planes of atoms in the crystal lattice. When one of the harmonics of this perturbation coincides with the energy difference between the actual electronic state of the ion and some other state, a transition can occur connecting both states. This is the well-known resonant-coherent excitation (RCE).

The RCE was first experimentally observed in a set of elegant experiments by Datz *et al.* [1–4], who first observed this effect through the reduction in the transmission of fixed-charge-state hydrogenic ions of atomic number $Z_1 = 5$–9, axially channeled in Au and Ag crystals, when the condition of resonance stated above was satisfied between the electron ground state and some excited state, the latter being more easily ionizable than the former due to stronger interaction with the solid. RCE has been observed under both axial [1–3] and planar [4] channeling conditions.

When ions of large atomic number are considered (e.g., Mg^{11+}), they have chances to leave the medium after suffering RCE without further ionization, so leading to emission of x rays, which have been experimentally detected and proved to be polarized in a way related to the channel geometry and the ion trajectory [5].

A first-principles quantitative study of this effect is presented in this Letter, based upon a numerical solution of the Schrödinger equation.

The interaction between the moving ion and the crystal can be separated into two distinct contributions to the total potential V: (a) static crystal potential V^C and (b) induced potential V^I.

(a) The crystal potential consists of the interaction with all electrons and nuclei in the unperturbed medium. The spatial periodicity of the lattice in which those are placed is experienced by the moving ion as a periodicity in time, which enables an electron bound to it to suffer transitions of frequency corresponding to the different harmonics contributing to the crystal potential. Experimental evidence exists that some frequencies can be suppressed due to interference effects [6]. For ions channeled in a {001} planar channel of an fcc crystal, the crystal potential can be written in terms of its oscillatory Fourier components V^C_{kl} of frequencies

$$\omega_{kl} = 2\pi v\gamma/a(k\cos\varphi + l\sin\varphi), \qquad (1)$$

where φ represents the angle between the ion velocity v and the [100] direction, γ stands for the relativistic Lorentz factor, a is the lattice constant, and k and l are integers such that $k + l$ is an even number. One has $V^C = \sum_{kl} V^C_{kl} e^{-i\omega_{kl}t}$. We will focus on this particular trajectory; the generalization to axial and surface channeling adds no extra conceptual difficulty.

(b) The induced potential results from the distortion produced in the medium by the projectile. The well-known wake potential corresponds to the part of the induced potential related to the perturbation of valence band electrons [7–9].

The whole RCE picture incorporates the following ingredients: (i) transitions connecting electronic bound states of the ion via frequencies of the crystal potential; (ii) splitting and mixing of electron states, originating in the net electric field derived from both the induced wake potential and the averaged (over the ion trajectory) crystal potential [10,11]; (iii) electron loss due to coherent excitation to the continuum; (iv) noncoherent electron-electron collisions leading to electron (de)excitation and electron loss; and (v) the ion trajectory, which accompanies the dynamical evolution of electron states. Electron capture from inner shells of target atoms may be important as well when the ion finds itself traveling very close to any

 0031-9007/96/76(11)/1856(4)$10.00

atomic plane of the crystal—that is, in the region where the strong interaction with target atoms leads to very high ionization rates, and, therefore, electron capture will be dismissed in this work.

(i) RCE can be regarded as an elastic process in the laboratory frame, in which the lattice acts like a source of momentum. In order to take place, RCE requires that the energy difference between bound states lies near some of the harmonic energies $\hbar\omega_{kl}$ of the crystal potential. The effect of the rest of the harmonics is negligible.

(ii) The electronic states of the ion are mixed and energy split by interaction with the target. The new basis of adiabatic states $|\phi_\lambda\rangle$, among which RCE can occur, change along the trajectory, because the interaction potential depends on the ion-atomic planes separation. By adiabatic states we understand those that diagonalize the continuous interaction potential, that is,

$$\sum_\beta V_{\alpha\beta} a_\beta^\lambda = (E_\lambda - \hbar\epsilon_\alpha) a_\alpha^\lambda , \tag{2}$$

where a_α^λ is the projection of perturbed state $|\phi_\lambda\rangle$ (of energy E_λ) onto unperturbed state $|\alpha\rangle$ (of energy $\hbar\epsilon_\alpha$), $V_{\alpha\beta} = -\langle\alpha|V^I + \overline{V^C}|\beta\rangle$, and $\overline{V^C} = \sum_{\omega_{kl}=0} V_{kl}^C$ is the so-called continuous planar potential [12,13].

(iii) RCE can take place in such a way that the excited state lies in the continuum, leading to electron loss [14–16]. The bound states can be depopulated via this effect, introducing in this way a width to the electronic adiabatic levels. It has been speculated that, for the case of surface channeling, the electron emitted in this way should travel with well-defined energy around preferential directions [16]. Experimental evidence of this type of electron emission is still lacking. For planar channeling, when very thin films and large projectile velocities are contemplated, the ejected electron may have a mean free path against the solid comparable to the film thickness, so that it may leave the target carrying direct information on the excitation process.

(iv) The excitation of target electrons and plasmons needs to be considered as well—the simultaneous promotion of the moving bound electron can occur by absorbing energy out of the fast ion motion. These kinds of inelastic collisions constitute a relevant mechanism of both excitation and ionization of the ion, as shown by Datz *et al.* [17]. Actually, these processes are well known in the field of charge states of ions traversing solids: They are the so-called Auger excitation and loss, respectively [14,15,18].

(v) The ion moves following a nearly classical trajectory, which is governed by the crystal planar potential (together with the image potential in the case of surfaces [16]). Moreover, since the trajectory forms a glancing angle with respect to the channel, the motion perpendicular to the crystal planes can be decoupled from the fast motion along the remaining "parallel" (to the channel) directions. Besides, the electron evolves nonadiabatically, in the sense that the excited electron wave function retains during long times (of the order of the period of the trajectory oscillations in the channel) the character of the original adiabatic state to which it was promoted.

The above considerations permit us to study the evolution of the electronic states of the ion by solving the Schrödinger equation, written in the form of coupled channel equations [19]. The explicit dependence on the amplitudes of free electronic states can be eliminated if one assumes low ionization rates. In its place, one finds extra coupling rates that will be denoted Γ. The remaining system of equations describes the time evolution of the amplitudes a_α of bound states $|\alpha\rangle$ as

$$i\hbar \frac{da_\alpha}{dt} = \sum_\beta \Sigma_{\alpha\beta} a_\beta + \sum_{\beta,kl} V_{\alpha\beta,kl}^{\text{crystal}} e^{i(\epsilon_\alpha - \epsilon_\beta - \omega_{kl})t} a_\beta , \tag{3}$$

where

$$\Sigma_{\alpha\beta} = V_{\alpha\beta} - \frac{i\hbar}{2}(\Gamma_{\alpha\beta}^{\text{CL}} + \Gamma_{\alpha\beta}^{\text{Auger}}) \tag{4}$$

represents complex self-energy matrix elements. The resonant term $V_{\alpha\beta,kl}^{\text{crystal}} = \langle\alpha|V_{kl}^C|\beta\rangle$ connects states $|\alpha\rangle$ and $|\beta\rangle$ via the harmonic (k,l) of the crystal potential [see point (a) above]. Here, the rates $\Gamma_{\alpha\beta}$ account for the leaking of electron probability coming from both coherent excitation to the continuum [i.e., coherent loss, $\Gamma_{\alpha\beta,kl}^{\text{CL}}$; see point (iii) above] and incoherent Auger processes [$\Gamma_{\alpha\beta}^{\text{Auger}}$; see point (iv) above]. The latter can be in turn divided into Auger loss (AL) and Auger (de)excitation (AE) to different bound states: $\Gamma_{\alpha\beta}^{\text{Auger}} = \Gamma_{\alpha\beta}^{\text{AL}} + \Gamma_{\alpha\beta}^{\text{AE}}$. Notice that whenever an Auger transition takes place, the target quantum state changes—so one can no longer sum amplitudes, as in Eq. (3). A way to handle this consists in convoluting the electron probability of jumping to a given bound state at every point of the ion trajectory with that solution of Eq. (3) derived by considering the new bound state as the initial condition at that particular point.

A dielectric formalism has been followed to obtain both the induced wake potential and the Auger matrix elements [15]. Use has been made of the random-phase approximation dielectric function [20] corresponding to a homogeneous electron gas of density equal to the average over the ion trajectory along several target atom spacings. The crystal potential has been calculated summing up contributions coming from all target atoms in the Ziegler, Biersack, and Littmark approximation, as has been already done in the theory of RCE at surfaces [16]. For the sake of simplicity, the excited states will be restricted to those of the L shell from now on.

Figure 1 shows the energy difference between ground and excited states for 25 MeV/amu Mg^{11+} ions channeled in a {001} planar channel of a Ni crystal, obtained from

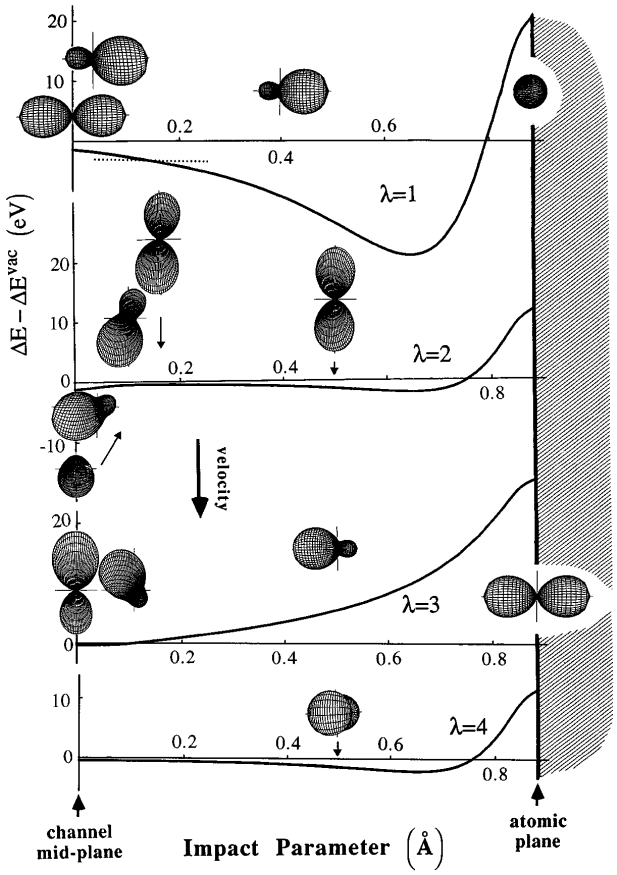

FIG. 1. Transition energies between the $|1s\rangle$ state and the hybrid adiabatic states of the L shell of a 25 MeV/amu Mg^{11+} ion moving parallel to a {001} planar channel of a Ni crystal as a function of distance from the channel midplane (impact parameter). The energy differences ΔE are given relative to the vacuum value $\Delta E^{\rm vac}$. The shape of the electronic cloud of the different excited states is shown for various positions in the channel by means of the accompanying insets. They represent the radial integral of the squared electron wave function. The ion moves from top to bottom. A dotted horizontal bar has been drawn for the state labeled $\lambda = 1$ to represent the harmonic energy $\hbar\omega_{2,0}$ corresponding to an angle $\varphi = 26.2°$ with respect to the [100] direction, according to Eq. (1).

Eq. (2). The shape of the four adiabatic states of the L shell is shown in the insets. Notice that state $\lambda = 1$ is oriented towards the channel wall, and, consequently, it can be more easily populated by RCE than the rest [5]. The dotted horizontal bar corresponds to the harmonic energy $\hbar\omega_{2,0}$ obtained from Eq. (1) for $\varphi = 26.2°$. The resonance condition $\hbar\omega_{2,0} = E_\lambda - E_{1s}$ can only be fulfilled for state $\lambda = 1$. No other low-index harmonics (k, l) lie near the energy range considered in the figure.

Under the same conditions as in Fig. 1, the impact-parameter dependence of transition rates involved in Eq. (4) are represented in Fig. 2 in order to illustrate the interplay between coherent ($\Gamma^{\rm CL}$, solid curves) and Auger ($\Gamma^{\rm AL}$, dashed curves) electron loss mechanisms: Incoherent Auger processes are dominant near the channel

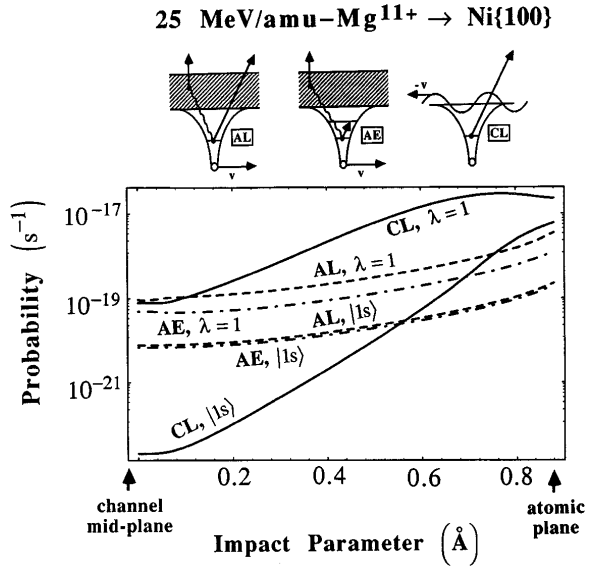

FIG. 2. Impact-parameter dependence of the transition rates involving states $|1s\rangle$ and $\lambda = 1$. $\Gamma^{\rm CL}$ (coherent-loss, solid curves), $\Gamma^{\rm AL}$ (Auger loss, dashed curves), and $\Gamma^{\rm AE}$ (Auger excitation, dot-dashed curves) are calculated under the same conditions as in Fig. 11. Insets are intended to show schematically the processes under consideration.

midplanes, whereas coherent ionization dominates in the vicinity of the atomic walls. The rate of Auger excitation is also shown for completeness ($\Gamma^{\rm AE}$, dot-dashed curves).

When the bound electron is originally prepared in state $|1s\rangle$ at point I of the trajectory schematically shown in the inset of Fig. 3, numerical evaluation of Eq. (3) shows that the probability of finding it in the same state at point

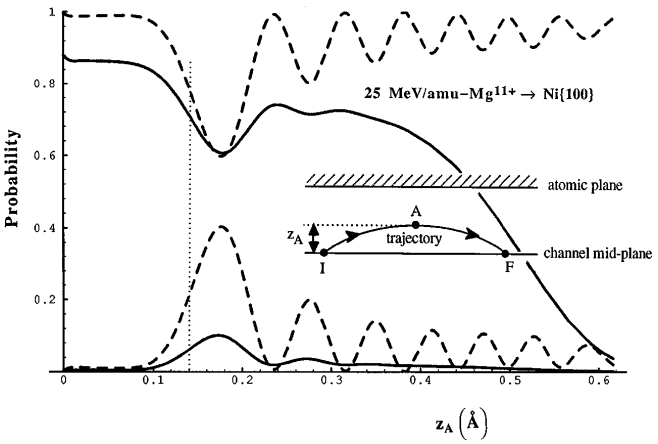

FIG. 3. Upper curves: Probability that an electron prepared in the ground state of a Mg^{11+} ion at position I of the trajectory sketched in the inset survives in that state at position F as a function of the amplitude of the trajectory z_A, under the same conditions as in Fig. 1. Lower curves: Probability of finding the electron in the L shell at point F. Solid (broken) curves represent the result obtained with (without) including coherent-loss and Auger processes [Γ terms in Eq. (4)]. The angle with respect to the [100] direction has been taken as $\varphi = 26.2°$.

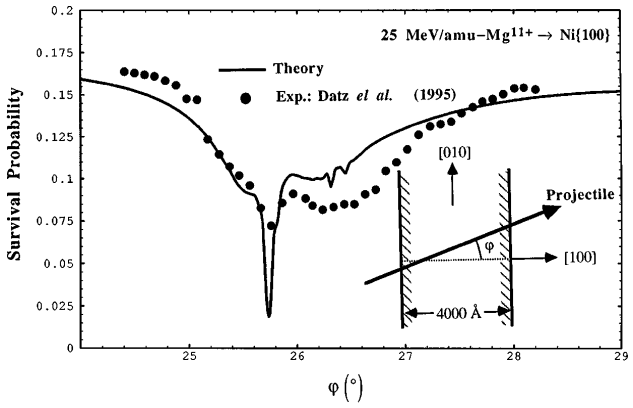

FIG. 4. Survival fraction of 25 MeV/amu Mg^{11+} ions after passing through a {001} planar channel of a 4000 Å thick Ni single crystal. φ is the angle between the velocity and the [100] direction. The inset represents a top view of the channel. The faces of the crystal are perpendicular to that direction. Solid line: present theory, multiplied by a factor of 0.3 to fit the experimental point corresponding to $\varphi = 28°$. Circles: experiment (Datz *et al.*, Ref. [5]).

F depends on the trajectory amplitude z_A as plotted in Fig. 3 (upper curves). Solid (broken) curves represent the result obtained with (without) including rates Γ in Eq. (4). Lower curves stand for the probability of finding the electron in the L shell at point F. Each point of the curves corresponds to a different trajectory amplitude. A vertical dotted line indicates the amplitude for which the condition of resonance between ground state and state $\lambda = 1$ [Eq. (1); see Fig. 1] is fulfilled at the turning point (point A). The oscillations observed in the figure are familiar in the study of potential-curve crossing in low-energy ion collisions [21]. The maxima (minima) in the oscillations occur for those amplitudes in which the contribution to the coherent excitation in the path from point I to A is in phase (completely out of phase) with respect to the contribution from A to F.

Finally, Fig. 4 represents the probability that a Mg^{11+} ion survives after crossing a thin Ni film as shown in the inset (i.e., Mg^{11+} fraction on exit). By changing the angle within the planar channel, one tunes the energy of resonance according to Eq. (1), giving rise to the structure shown in the figure. In order to compare the present theory with available experimental data (black points, Ref. [5]) the calculated result has been multiplied by a factor of 0.3 to fit the experimental point corresponding to $\varphi = 28°$. This quantitative disagreement might be due to an underestimate of the range of Auger rates for target inner shells, connected with the local density approximation employed here. In the calculation, the beam has been considered to enter the film parallel to the channel planes with no divergence. An average over initial impact parameters has been performed.

In summary, electron intraionic processes and electron loss taking place in fast planar-channeled ions are shown to receive contributions from both coherent and incoherent mechanisms. The former, dominant in the vicinity of the channel walls, is due to coherent interaction with the static crystal potential, while the latter, dominant in the channel midplanes, involves inelastic electron-electron collisions via the dynamically screened interaction. Moreover, the impact-parameter dependence of the mixing and energy splitting of electronic states of the ion, originating in the perturbation exerted by the solid on the bound electron, determines, together with the time evolution of the basis of adiabatic states along the ion trajectory, the magnitude of the RCE effect; this oscillates with the amplitude of the trajectory oscillations in the channel. Finally, reasonable agreement is found between this theory and experiment.

The authors want to thank V. H. Ponce and A. Salin for helpful and enjoyable discussions. Help and support is acknowledged from the Departamento de Educación del Gobierno Vasco, Gipuzkoako Foru Aldundia, CAICYT, and Iberdrola S. A.

[1] S. Datz *et al.*, Phys. Rev. Lett. **40**, 843 (1978).
[2] C. D. Moak *et al.*, Phys. Rev. A **19**, 977 (1979).
[3] S. Datz, J. Phys. (Paris), Colloq. **40**, C1-327 (1979).
[4] S. Datz *et al.*, Nucl. Instrum. Methods Phys. Res. Sect. B **170**, 15 (1980).
[5] S. Datz *et al.*, Nucl. Instrum. Methods Phys. Res. Sect. B **100**, 272 (1995).
[6] H. F. Krause *et al.*, Phys. Rev. Lett. **71**, 348 (1993).
[7] J. Neufeld and R. H. Ritchie, Phys. Rev. **98**, 1632 (1955); Phys. Rev. **99**, 1125 (1955).
[8] P. M. Echenique, R. H. Ritchie, and W. Brandt, Phys. Rev. B **20**, 2567 (1979).
[9] F. J. García de Abajo and P. M. Echenique, Phys. Rev. B **48**, 13 399 (1993); Phys. Rev. B **46**, 2663 (1992).
[10] O. H. Crawford and R, H. Ritchie, Phys. Rev. A **20**, 1848 (1979).
[11] J. P. Rozet *et al.*, Phys. Rev. Lett. **58**, 337 (1987).
[12] S. Datz *et al.*, Phys. Rev. **179**, 315 (1969).
[13] F. Abel *et al.*, Phys. Rev. B **13**, 993 (1976).
[14] F. Sols and F. Flores, Phys. Rev. B **30**, 4878 (1984).
[15] P. M. Echenique, F. Flores, and R. H. Ritchie, Solid State Phys. **43**, 229 (1990).
[16] F. J. García de Abajo, V. H. Ponce, and P. M. Echenique, Phys. Rev. Lett. **69**, 2364 (1992); Phys. Rev. B **49**, 2832 (1994).
[17] S. Datz *et al.*, Radiat. Eff. Defects Solids **117**, 73 (1991).
[18] F. Guinea, F. Flores, and P. M. Echenique, Phys. Rev. Lett. **47**, 604 (1981).
[19] O. E. Krivosheev and Y. L. Pivovarov, JETP Lett. **56**, 240 (1992).
[20] J. Lindhard and K. Dan, Vidensk. Selsk. Mat. Fys. Medd. **28**, No. 8 (1954).
[21] J. B. Delos and W. R. Thorson, Phys. Rev. A **6**, 728 (1972).